THE JOURNAL OF PHYSICAL CHEMISTRY A

© Copyright 2000 by the American Chemical Society VOLUME 104, NUMBER 22, JUNE 8, 2000

FEATURE ARTICLE

Ab Initio Multiple Spawning: Photochemistry from First Principles Quantum Molecular Dynamics

M. Ben-Nun, Jason Quenneville, and Todd J. Martínez*

Department of Chemistry and The Beckman Institute, University of Illinois, Urbana, Illinois 61801

Received: November 23, 1999; In Final Form: March 2, 2000

The ab initio multiple spawning (AIMS) method is a time-dependent formulation of quantum chemistry, whereby the nuclear dynamics and electronic structure problems are solved simultaneously. Quantum mechanical effects in the nuclear dynamics are included, especially the nonadiabatic effects which are crucial in modeling dynamics on multiple electronic states. The AIMS method makes it possible to describe photochemistry from first principles molecular dynamics, with no empirical parameters. We describe the method and present the application to two molecules of interest in organic photochemistry—ethylene and cyclobutene. We show that the photodynamics of ethylene involves both covalent and ionic electronic excited states and the return to the ground state proceeds through a pyramidalized geometry. For the photoinduced ring opening of cyclobutene, we show that the disrotatory motion predicted by the Woodward−Hoffmann rules is established within the first 50 fs after optical excitation.

I. Introduction

Thanks to the efforts of many workers over the past few decades, quantum chemistry can be considered a mature discipline. The wide usage of quantum chemical programs outside of chemistry and the award of the 1998 Nobel Prize in Chemistry are evidence of this. Where are the remaining frontiers? The vigorous activity of many quantum chemistry research groups suggests that the answer to this question is multifaceted and would require several articles. We do not make any attempt at a complete answer here. However, we do aim to persuade the reader that one important facet of this answer is time-dependent quantum chemistry. Furthermore, the confluence of theoretical advances along this front with recent experimental developments in ultrafast spectroscopy provides a unique opportunity to understand photochemistry at a level of detail that has been heretofore impossible. We begin with an intentionally strongly biased recounting of some milestones in quantum chemistry, highlighting the direction in its development that leads naturally to the explicit introduction of time into quantum chemistry.

The implementation of analytic energy gradients[1,2] was a major milestone in the development of quantum chemistry. Before this time, theoretical chemists were forced to guess molecular geometries, extract them from limited resolution X-ray crystallography studies, or combine these approaches with the optimization of a selected few degrees of freedom. All of these options had the disadvantage of imposing the theoretician's structural preconceptions on the molecule of interest. With the availability of analytic energy gradients, it became a routine matter to largely avoid such preconceptions and assumptions by directly optimizing all of the molecular degrees of freedom to find equilibrium structures. Furthermore, this paved the way for a second milestone—the introduction of generally applicable numerical methods[3,4] to trace the intrinsic reaction coordinate[5] (IRC) connecting reactants and products. With automatic procedures to find equilibrium structures of reactants and

10.1021/jp994174i CCC: $19.00 © 2000 American Chemical Society
Published on Web 05/16/2000

products and to follow the IRC, mechanistic pathways for chemical reactions can be found with few assumptions.

Yet the desired connection between electronic structure theory and chemical reactivity remains incomplete. Despite its theoretical importance, the IRC is not a physical pathway that molecules can follow! Paradoxically, it is only in the limit of infinite friction that any molecule could follow the IRC—the same limit where activated chemical reactions are impossible. The missing ingredient is of course the nuclear kinetic energy, traditionally considered the domain of molecular dynamics. Such considerations led to the reaction path Hamiltonian (RPH) approach.[6] By combining local information about the potential energy surface (PES) along the IRC and molecular dynamics, the RPH method offers a theoretical framework that can provide a detailed description of chemical reactivity while avoiding statistical assumptions and tedious analytic fits of potential energy surfaces.[7−10] However, application of the RPH method has been fairly limited, largely because of the technical difficulties associated with the required coordinate transformations.

All of the aforementioned developments were steps toward allowing molecules to tell us where they wanted to go and how they wanted to get there, i.e., a first principles description of chemical reactivity. Even so, a separation between the electronic and nuclear problems is still enforced to some degree. This separation is largely a reflection of the existence of two independently developed subfields in theoretical chemistry—quantum chemistry and molecular dynamics. Historically, the prevailing model has been that quantum chemistry provides potential energy surfaces. The desired connections to chemistry are then either inferred, established by invoking statistical rate theories, or sometimes made explicit by potential energy surface fitting and dynamical simulation. Instances of the latter have usually been carried out through collaborative efforts, although there are notable exceptions (for example, refs 11−15). The first challenges to this model came from dynamicists, under the rubric of "ab initio molecular dynamics (AIMD)." The idea was to recompute the potential energy surface "on-the-fly," using ab initio quantum chemistry, as needed by molecular dynamics. The first attempt of which we are aware came from Leforestier[16] in a paper with a surprisingly early publication date. Computational difficulties hampered progress for many years, and the next major development again came from the dynamics community in the form of the Car−Parrinello method.[17] Encouraged by the successes of the Car−Parrinello method, much work has been devoted to making AIMD practical and significant progress has been made.[18−28] However, with only a few recent exceptions,[29,30] AIMD methods aimed at real-time dynamics consider the nuclei to be purely classical. This assumption is completely natural and appropriate for many chemical reactions, particularly those occurring entirely on the ground state and not involving proton or electron transfer. Yet, much of the chemistry that satisfies these requirements also involves large activation barriers. The short simulation time scale afforded by the solution of the electronic structure problem "on-the-fly" thus poses a serious difficulty. This difficulty remains, although it has been ameliorated to some extent by increases in computational power, a careful choice of the problems where ab initio molecular dynamics is applied, and techniques for simulation of rare events.[31−34]

One branch of chemistry where much of the interesting behavior occurs on very short time scales is photochemistry. It was recognized early on that the excited state dynamics often occurred on a short time scale, but exactly how short this time scale is has only become apparent in the past decade. In many cases, the excited state dynamics is essentially complete within 1 ps, as established by femtosecond spectroscopy.[35] Photochemistry is therefore a natural area for application of ab initio molecular dynamics for two major reasons. First, the relevant time scales are often very short and the experiments that can probe these time scales are now available. Thus, both the experimental impetus and the theoretical feasibility are here. Second, in contrast to ground electronic states, the electronic structure of excited states is not well understood. Thus, this direction provides a partial refocusing of ab initio molecular dynamics as a tool to understand electronic structure—we can use the nuclear dynamics to identify the interesting parts of the potential energy surface. The electronic structure that gives rise to the potential energy surfaces can then be studied in more detail in the context of the coordinates that the dynamics indicates to be most important.

There are two main obstacles to overcome in the development of an ab initio molecular dynamics description of photochemistry. First, the electronic problem must be solved efficiently and accurately for both ground and excited electronic states. Second, the quantum mechanical character of the nuclear dynamics must be addressed because at least two electronic states will be involved during the dynamics. We first describe the approaches we have taken to solve these problems (section II) and then present the results of two recent applications in organic photochemistry (Section III).

II. Theory

1. Excited State Electronic Structure. The electronic structure of excited states already poses difficulties for conventional time-independent quantum chemistry. The causes of the problem are strong multireference character in many excited state wave functions and an increased importance (relative to ground states) of electron correlation effects. The excited states that are most prominent in electronic absorption spectra are generally dominated by single excitations and often have considerable single-reference character. Thus, methods such as configuration interaction singles[36,37] (CIS) can provide reasonable estimates for the vertical excitation energies to these states. However, the usefulness of single-reference methods in general, and single-reference/single-excitation methods in particular, rapidly diminishes when global properties of the excited state PES are required. There are two important problems. First, electronic states with doubly excited character cannot be modeled accurately with CIS. Although these states are usually optically forbidden and hence unimportant for the electronic absorption spectrum, they can play a significant role in photochemistry. Second, the excited state manifold often contains avoided crossings and conical intersections. Near these regions of the PES, the wave function rapidly changes character and a multireference description becomes necessary—even if the wave functions for each of the interacting states are reasonably described by a single configuration outside the crossing/intersection region. Single-reference methods will have great difficulty describing the surface equally well in the midst of these changes. Thus, for example, the CIS method fails to predict the correct global minimum on the lowest valence adiabatic excited state surface of ethylene, vide infra.

The first principles treatment of photochemistry requires the repeated solution of the electronic Schrödinger equation for multiple electronic states, including the nonadiabatic coupling that induces transitions between states. At the same time, there is no point in carrying out a first principles approach if the underlying potential energy surfaces are not at least qualitatively

accurate. The conflicting requirements of accuracy and efficiency, which are already present in time-independent quantum chemistry, are made more severe in the time-dependent case because of the sheer number of PES computations that are required and the need for global accuracy in the PESs. Despite the computational advantages, most single-reference methods are not appropriate because of their difficulty in providing this global accuracy, i.e., in predicting the correct shape of the excited state potential energy surface(s). It is currently unknown to what extent this criticism applies to excited state extensions of density functional theory,[38−40] which are superficially similar to single-reference/single-excitation methods. Although these excited state density functional methods present a promising avenue for future exploration, application in the current context may be premature.

A further problem in treating excited states lies in avoiding a variational bias to the ground electronic state. State averaging has been proposed as a means to cure this defect,[41−44] where the orbitals are determined to minimize a weighted average of the ground and one or more excited state energies. The resulting orbitals are not optimal for any of the target electronic states, but are rather a "best-compromise" set. The simplest way to allow for state-dependent orbital relaxation is through the inclusion of single excitations in a configuration interaction (CI) wave function. In this scheme, single excitations should be taken from the same set of reference configurations that are used to determine the orbitals in the state-averaged multiconfiguration SCF (MCSCF). A similar strategy has seen considerable success in past treatments of excited states. For example, the first-order CI method of Schaefer[45] and the POL-CI method of Goddard[46] are both variants of this technique.

Occupation averaging has aims similar to those of state averaging, but is computationally slightly simpler. In this approach, the orbitals which are of variable occupancy in the ground and excited states are equally populated with electrons. For example, in the case of $\pi \rightarrow \pi^*$ excitation of ethylene, the π and π^* orbitals would each be singly occupied. There are several ways to accomplish this, differing in the treatment of electronic spin coupling. Perhaps the simplest is to take the orbitals from a triplet single-determinant wave function. This approach has precedent for ethylene, where the lowest triplet Hartree−Fock wave function is less prone than the ground state singlet wave function to overemphasize Rydberg character in the orbitals and hence has been argued to provide a better starting point for CI expansions.[47] A more sophisticated approach is to determine the orbitals within the framework of a generalized valence bond (GVB) wave function[48] where the covalent and ionic states are constrained to have equal weights. For example, the GVB(1/2) wave function for ethylene would be

$$\psi_{\mathrm{GVB(1/2)}} = c_{\mathrm{cov}}\hat{A}(\psi_{\mathrm{core}}(\chi_{\mathrm{Cp,r}}\chi_{\mathrm{Cp,l}} + \chi_{\mathrm{Cp,l}}\chi_{\mathrm{Cp,r}})(\alpha\beta - \beta\alpha)) + c_{\mathrm{ion}}\hat{A}(\psi_{\mathrm{core}}(\chi_{\mathrm{Cp,r}}\chi_{\mathrm{Cp,r}} + \chi_{\mathrm{Cp,l}}\chi_{\mathrm{Cp,l}})(\alpha\beta - \beta\alpha)) \quad (2.1)$$

where $\hat{A}$ is the antisymmetrizing operator, ψ_{core} represents all the electrons in the σ framework, and $\chi_{\mathrm{Cp,r}}$ and $\chi_{\mathrm{Cp,l}}$ denote the nonorthogonal GVB orbitals on the right and left carbon atoms which are dominated by contributions from the *2*p atomic orbitals of the carbon atoms. As is well-known, this wave function can be written in an equivalent form built from the orthogonal molecular orbitals:

$$\psi_{\mathrm{GVB(1/2)}} = c_{\mathrm{b}}\hat{A}(\psi_{\mathrm{core}}\phi_\pi\phi_\pi(\alpha\beta - \beta\alpha)) + c_{\mathrm{a}}\hat{A}(\psi_{\mathrm{core}}\phi_{\pi^*}\phi_{\pi^*}(\alpha\beta - \beta\alpha)) \quad (2.2)$$

The usual GVB wave function would optimize both the orbitals and the coefficients c_{cov}, c_{ion} or, equivalently, c_{a}, c_{b}. Occupation-averaged orbitals appropriate for the GVB wave function can be defined to minimize the average energy of the individual terms in eq 2.2:

$$E_{\mathrm{average}} = (1/2)[E(\psi_{\mathrm{core}}\phi_\pi\phi_\pi) + E(\psi_{\mathrm{core}}\phi_{\pi^*}\phi_{\pi^*})] \quad (2.3)$$

This is theoretically somewhat more appealing than the use of triplet orbitals, because the orbitals in this case are derived from a wave function averaged over states with the desired singlet spin coupling. However, we have found little difference in studies on ethylene. The subsequent CI expansion is apparently sufficiently flexible to correct the shape of the orbitals in either case. For example, the global features of the potential energy surfaces are qualitatively unchanged for these two choices of starting orbitals, and even the vertical excitation energies are within 0.1 eV of each other. Our previous study on ethylene[49] has used the GVB-occupation-averaged (GVB-OA) orbitals, but we use the simpler Hartree−Fock-occupation-averaged (HF-OA) orbitals (with high spin coupling) in what follows. In either case, the set of reference configurations from which single excitations are drawn in the subsequent CI expansion is of the complete-active-space (CAS) type, allowing all possible configurations of the active electrons in the occupation-averaged orbitals that are consistent with the Pauli exclusion principle. We refer to this form of wave function as HF-OA-CAS(*n*/*m*)*S or GVB-OA-CAS(*n*/*m*)*S, respectively, where n and m denote the number of electrons and orbitals in the active space which defines the reference configurations. The S indicates that single excitations are taken from the CAS(*n*/*m*) reference configurations.

A final issue is the size of the one-electron basis set. The calculations presented here use double-ζ quality basis sets, which is the minimum that can be expected to describe both ground and excited states simultaneously. Especially for small molecules and near the equilibrium geometry of the ground state, Rydberg states are often found among the low-lying excited states. Thus, inclusion of Rydberg basis functions would be desirable. Computational considerations make this impractical at present. In cases with little or no valence−Rydberg mixing, neglect of these basis functions is tantamount to assuming that the dynamics is diabatic with respect to the Rydberg manifold (i.e., the Rydberg states are spectators). Since the difference in size of the Rydberg and valence states is expected to lead to weak nonadiabatic coupling between them, this may be a reasonable assumption. While early theoretical studies of small unsaturated organic molecules, e.g., ethylene, often found extensive Rydberg−valence mixing,[50−54] the best current calculations suggest that this was largely an artifact.[47,55,56] Nevertheless, there will be some amount of mixing which our treatment ignores, and the effect of this approximation remains to be completely quantified.

To assess the accuracy of our wave function ansatz, we have computed the potential energy surface for the twisting and pyramidalization coordinates of ethylene. (The pyramidalization coordinate is defined as the angle between the CC axis and the bisector of the CH_2 plane; see Sketch I.) As discussed in more detail below, these are the coordinates that dominate the photodynamics in this molecule. Figure 1 shows the PESs which are obtained using the HF-OA-CAS(2/2)*S wave function with a double-ζ basis set. The benchmark calculations for comparison have been performed using the MOLPRO program.[57] We first determined a state-averaged CAS(2/6) wave function (equally weighting the three lowest electronic states) in the aug-cc-

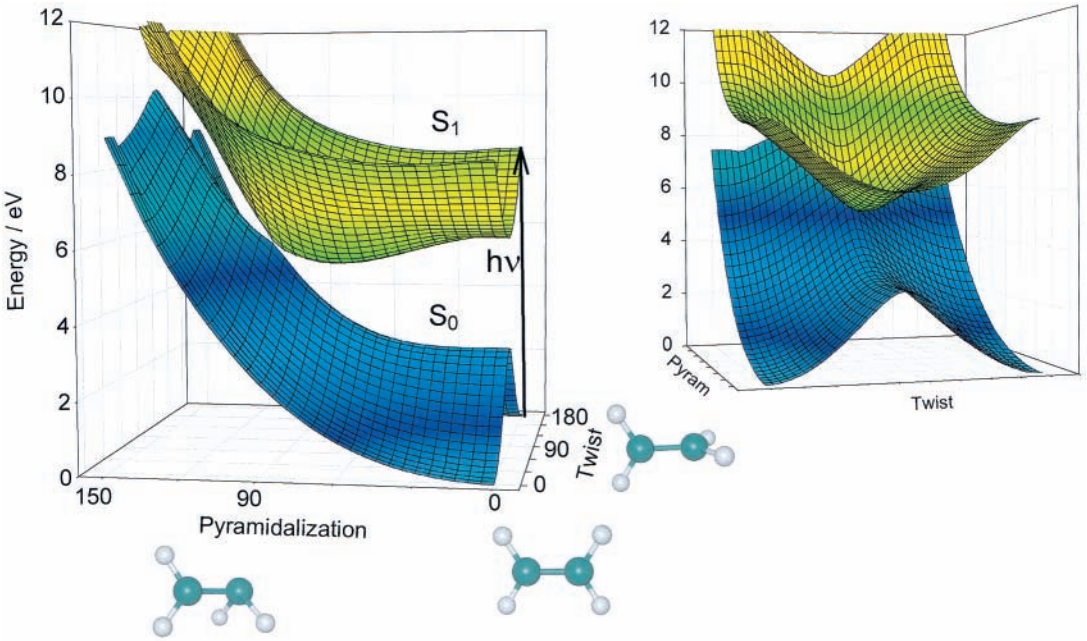

Figure 1. Two views of the ground and first excited electronic states of ethylene, computed using the OA-GVB-CAS(2/2)*S wave function, as a function of the pyramidalization and twist angles. (All other coordinates, except the CC bond distance, are kept at their ground state equilibrium value and the CC bond distance is stretched to 1.426 Å.) On the ground electronic state the molecule is planar (twist angle is 0° or 180°) and on the lowest excited state the twisted geometry (twist angle 90°) is a saddle point. Accessing the conical intersection requires pyramidalization of one of the methylene fragments. Note that the conical intersection is tilted and nearly coincides with the global minimum of the excited state PES (not shown).[39]

pVDZ[58] basis set. These orbitals were then used in an internally contracted[59−61] multireference single and double excitation CI

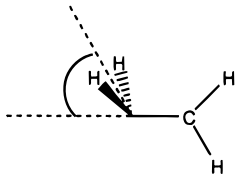

Sketch I

(MRSDCI), leading to a wave function with 653 735 contracted (2 791 010 uncontracted) configurations. The aug-cc-pVDZ basis set includes the diffuse functions that are essential to an accurate description of the Rydberg states. Furthermore, the SA-3-CAS(2/6)*SD wave function includes more extensive correlation than the simpler one used in the AIMS calculations described below. The resulting PESs for this more accurate wave function are shown in Figure 2. Comparison of Figures 1 and 2 shows that this more accurate method gives rise to the same qualitative features as our simpler wave function ansatz. The global minimum on the first excited state (not shown) is pyramidalized and twisted, and a conical intersection between the ground and first excited states lies in close proximity to the excited state minimum. The influence of the diffuse functions is most pronounced in the Franck−Condon region. The flat excited state PES of Figure 2 in this region corresponds to the 3s Rydberg state of ethylene, which has very low oscillator strength. The SA-6-CAS(2/6)*SD wave function provides a quantitatively accurate estimation of the vertical excitation energies—6.8 eV and 7.8 eV for excitation to the R(3s) and V states, respectively. These numbers can be compared to the experimental estimates of 7.16 and 8.0 eV, respectively.[62] The pyramidalization of the global minimum on the first excited state is in contrast to previous predictions[63] based on CIS computations, which instead find a global minimum for the D_{2d}

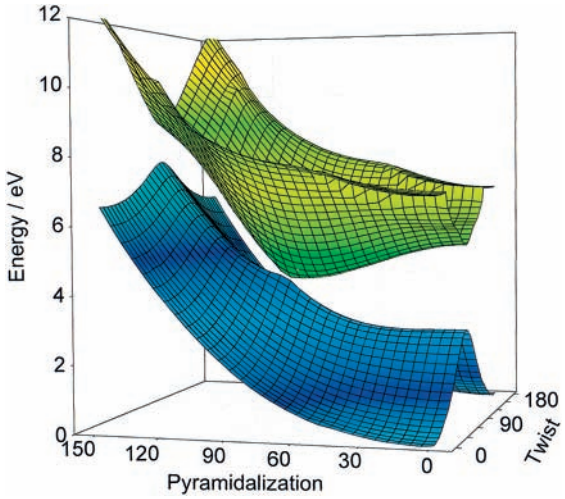

Figure 2. As in Figure 1, but computed using the aug-cc-pVDZ basis set and a state-averaged (equally weighting the lowest three states) CAS-(2/6) wave function augmented with single and double excitations [i.e., SA-3-CAS(2/6)*SD]. The form of the excited state PES is in agreement with the simpler model of Figure 1—in particular the global minimum of the lowest excited state remains pyramidalized.

twisted, nonpyramidalized structure. This could have been expected because of the poor treatment of the doubly excited state which dominates the wave function for pyramidalized geometries. We can conclude that the HF-OA-CAS(2/2)*S wave function provides ground and excited state potential energy surfaces with the correct global features. The vertical excitation energy predicted is in error by 1 eV, but this error is reduced to 0.2 eV when a single set of diffuse functions is included in the basis set.

A final electronic structure issue is the form of the coupling between electronic states. This depends on whether an adiabatic or diabatic representation has been chosen. The first of these diagonalizes the electronic potential energy, while the second

minimizes the change in electronic character due to nuclear perturbations and hence approximately diagonalizes the nuclear kinetic energy. While dynamicists have generally preferred the diabatic representation because it leads to smoother potential energy surfaces, these states are difficult to obtain without information about the electronic wave functions at various molecular geometries.[64,65] Hence, we prefer to work with adiabatic electronic states, in which case the form of the interstate coupling becomes

$$(\mathbf{d}^{IJ})_i = \left\langle \psi_I(\mathbf{r};\mathbf{R}) \left| \frac{\partial}{\partial R_i} \right| \psi_J(\mathbf{r};\mathbf{R}) \right\rangle_{\mathbf{r}} \tag{2.4}$$

where the parametric dependence of the electronic wave functions on the nuclear coordinates **R** is denoted by the semicolon and the integration is over the electronic coordinates **r**. For the electronic wave functions under consideration, this function has contributions from the geometry dependence of both the orbitals and the CI coefficients. The second term is usually dominant,[66,67] and the use of an averaging procedure to find the orbitals decreases the orbital contribution. Thus, we neglect the orbital contribution to the coupling function. The derivatives of the CI coefficients are found from numerical differentiation in our current implementation, but it is worth noting that the required theory for analytic evaluation has been presented in the literature.[44] In either case, it is crucial to adopt a consistent convention for the phase of the orbitals that is independent of molecular geometry.

2. Full Multiple Spawning Dynamics. To describe dynamics on excited electronic states, it is necessary to include quantum mechanical effects on the nuclei in addition to the quantum mechanical nature of the electrons that is incorporated during the generation of the potential energy surfaces and their couplings. This is simply because molecules generally live in the excited state manifold for a short time before returning to the ground electronic state. Often, this decay is mediated by conical intersections—points of true degeneracy between two electronic states.[68−70] Dynamics on multiple coupled potential energy surfaces is therefore required, but this does not admit a description in terms of purely classical mechanics. On the other hand, multielectronic state dynamics is formally straightforward in the context of quantum mechanics.[71]

An immediate problem arises when one considers a merger of quantum chemistry and quantum dynamics. While quantum dynamics is global, requiring the entire potential energy surface at each time step, quantum chemistry is local—given a specific nuclear geometry it provides the potential energy and its derivatives. The method chosen for the dynamics must therefore be compatible with the locality of quantum chemistry. The computational expense of quantum chemistry makes it paramount that the dynamical method be as much as possible of a local nature, requiring at every time step information about the current values of the potential energy surface and its derivatives at specific (as few as possible) nuclear configurations. Classical mechanics provides an ideal match as it only requires the current values of the forces, but it is limited to describing the dynamics of heavy particles occurring on a single electronic state. Therefore, we will require a dynamical method that retains a classical flavor while allowing for quantum mechanical effects, e.g., interaction of nuclear population of different electronic states.

The full multiple spawning (FMS) method uses classical mechanics to generate a basis set within which the nuclear Schrödinger equation is solved.[72−75] The basis functions are chosen to be of the frozen Gaussian form that was originally introduced by Heller in "frozen Gaussian approximation" (FGA) dynamics.[76] Since its introduction in the mid-1970s, Heller's Gaussian wave packet dynamics algorithm has been successful in describing a number of short time processes (see, e.g., the earlier work of Heller et al.[77−80] as well as more recent work[81−87]). Importantly, and unlike the original FGA method, the complex coefficients of the nuclear basis functions are fully coupled. Thus, the only approximation at this point is the use of a finite basis set. More specifically, a multiconfigurational frozen Gaussian nuclear wave function of the form

$$\Psi = \sum_I \chi_I(\mathbf{R};t)|I\rangle \tag{2.5}$$

is used for a problem with any number of nuclear and electronic degrees of freedom. In eq 2.5 each component is a product of a time-dependent nuclear wave function, $\chi_I(\mathbf{R};t)$, and an electronic wave function, $|I\rangle$. The latter is allowed to depend parametrically on the nuclear coordinates (**R**), and in what follows we use bold letters to denote vectors and matrices. The time-dependent nuclear wave function, for each electronic state, is represented as a linear combination of multidimensional traveling Gaussian basis functions with time-dependent coefficients

$$\chi_I(\mathbf{R};t) = \sum_j C_j^I(t)\, \chi_j^I(\mathbf{R};\bar{\mathbf{R}}_j^I(t),\bar{\mathbf{P}}_j^I(t),\bar{\gamma}_j^I(t),\alpha_j^I) \tag{2.6}$$

Here, the indices j and I label the jth nuclear basis function on electronic state I, and all the time dependencies of the basis set are explicitly denoted. A one-dimensional Gaussian basis function is associated with each nuclear degree of freedom so that each of the multidimensional Gaussian basis functions in eq 2.6 is constructed as a product of one-dimensional Gaussian basis functions

$$\chi_j^I(\mathbf{R};\bar{\mathbf{R}}_j^I(t),\bar{\mathbf{P}}_j^I(t),\bar{\gamma}_j^I(t),\alpha_j^I) = \mathrm{e}^{i\bar{\gamma}_j^I(t)} \prod_{\rho=1}^{3N} \tilde{\chi}_j^I(R_\rho;\bar{R}_{\rho j}^I(t),\bar{P}_{\rho j}^I(t),\alpha_{\rho j}^I)$$

$$\tilde{\chi}_j^I(R_\rho;\bar{R}_{\rho j}^I(t),\bar{P}_{\rho j}^I(t),\alpha_{\rho j}^I) = \left(\frac{2\alpha_{\rho j}^I}{\pi}\right)^{1/4} \exp[-\alpha_{\rho j}^I(R_\rho - \bar{R}_{\rho j}^I(t))^2 + i\bar{P}_{\rho j}^I(t)(R_\rho - \bar{R}_{\rho j}^I(t))] \tag{2.7}$$

where the index ρ enumerates the $3N$ Cartesian coordinates of the molecule. Each Gaussian is parametrized with a time-dependent position, momentum, and nuclear phase [$\bar{R}_{\rho j}^I(t)$, $\bar{P}_{\rho j}^I(t)$, $\bar{\gamma}_j^I(t)$, respectively] and a time-independent width ($\alpha_{\rho j}^I$). Hamilton's equations of motion govern the time evolution of the position and momentum parameters in each Gaussian, and the propagation of the single nuclear phase is determined in the usual semiclassical way as the time integral of the Lagrangian. This provides the desired connection to classical mechanics, and hence the compatibility with quantum chemistry. Because the optimal choice for the time-independent width is known only for the case of harmonic separable potentials,[76] we view it as a parameter characterizing the nuclear basis set.

The time evolution of the complex coefficients $C_j^I(t)$ is governed by the nuclear Schrödinger equation. Given the wave function ansatz of eqs 2.5−2.7 and using the orthonormality of the electronic wave functions, we obtain the following set of coupled equations of motion for these coefficients

$$\frac{dC_j^I(t)}{dt} = -i\sum_{k,l}(\mathbf{S}_{II}^{-1})_{k,l} \times \{(\mathbf{H}_{II} - i\dot{\mathbf{S}}_{II})_{k,l}C_l^I + \sum_{J\neq I}(\mathbf{H}_{IJ})_{k,l}C_l^J\} \quad (2.8)$$

Here, $\mathbf{S}_{II}$ and $\dot{\mathbf{S}}_{II}$ are the time-dependent nuclear overlap matrix and its time derivative: $(\mathbf{S}_{II})_{k,l} = \langle\chi_k^I|\chi_l^I\rangle$ and $(\dot{\mathbf{S}}_{II})_{k,l} = \langle\chi_k^I|(\partial/\partial t)\chi_l^I\rangle$. The subblock of the Hamiltonian matrix describing the inter state coupling between basis functions on electronic states I and J is $(\mathrm{H}_{IJ})_{k,l} = \langle\chi_k^I|\hat{\mathbf{H}}|\chi_l^J\rangle$.

Numerical integration of eq 2.8 requires (at each time step and for each nuclear basis function) the diagonal and off-diagonal elements of the Hamiltonian matrix. These include integrals over the potential energy surface or coupling between potential energy surfaces. For certain model problems it is sometimes possible to evaluate these multidimensional integrals analytically. However, when the PESs are known only locally, as in ab initio molecular dynamics, this is not possible and we have overcome this problem in AIMS by using saddle-point (SP) approximations of the required integrals.[49,88−90] These approximations are motivated by the localized nature of the nuclear basis functions and bear a strong resemblance to the Mulliken−Ruedenberg and related approximations which have been used in electronic structure theory for the approximate evaluation of multicenter two-electron integrals.[91] We have tested the SP approximations, with favorable results, for some model nonadiabatic problems.[72,88,92] Nevertheless, this is but an approximation (the first beyond the use of a finite nuclear basis set) and it can be improved using, for example, various forms of numerical quadrature. Even though these would require more computational effort, and are currently beyond our computational capabilities, they and other approximations (e.g., high order SP approximations) should certainly be investigated.

Further reduction in computational cost (which also resolves the dynamics into classical and nonclassical parts, thereby simplifying a classical interpretation of the resulting dynamics) can be obtained by invoking the ideas of operator splitting and Trotter factorization[93] (see ref 92 for a more comprehensive discussion). The split-operator propagation is another approximation which is however compatible with the saddle-point approximation.

In principle it is sufficient to say that the basis set consists of an infinite ensemble of trajectories (e.g., nuclear basis functions) on each electronic surface, each dressed by a multidimensional Gaussian function. However, such an implementation would be impractical. On the other hand, the fact that the basis functions move according to classical mechanics implies that certain quantum mechanical phenomena (e.g., nonadiabatic effects and tunneling) may not be well-described with a basis set of fixed size. Practical implementation of the method thus requires a criterion for adaptively expanding the size of the basis set. The algorithm that we use attempts to balance two contradicting requirements: maintaining a reasonable approximation to the exact nuclear wave function while minimizing the growth of the basis set size with time (and with the number of nuclear degrees of freedom). The basic idea of the spawning method is to control the growth of the basis set by allowing it to expand only when the dynamics signals impending failure of classical mechanics, e.g., nonadiabatic and/or tunneling effects. For multistate problems this is achieved by monitoring the magnitude of the nonadiabatic coupling for each nuclear basis function. When a nuclear basis function enters a region of strong nonadiabatic coupling, the solution of the nuclear Schrödinger equation is stopped and new basis functions are spawned (i.e., created), with zero initial population on the other electronic state. The initial position and momentum of the newly spawned basis function(s) are determined using Franck−Condon like considerations—they are chosen to have maximal overlap with their parent basis function at some point in time during the nonadiabatic event. Once the initial conditions (position and momentum) for the new basis functions are determined, the solution of the nuclear Schrödinger equation continues, including the trajectory amplitudes for the newly spawned basis function(s). Excessive growth of the nuclear basis set is avoided by rejecting spawning attempts that lead to linear dependence.

A pictorial description of the spawning algorithm is depicted in Figure 3 using a collinear A + BC → AB + C reaction. The right and left set of panels correspond to two diabatic potential energy surfaces (represented by blue contour lines), correlating to A + BC and AB + C, respectively. The two diabatic surfaces are coupled via a constant potential energy term, and they are plotted in Jacobi coordinates: the A to BC center-of-mass distance, R, and the BC distance, r. The nuclear wave functions are superimposed on the contour lines. The calculation begins with population on a single diabatic PES, uppermost left panel. As the basis functions approach the nonadiabatic region (atom A approaches the diatomic molecule and then recedes from it), new basis functions are created (i.e., "spawned") on the other diabatic state. The location of individual basis functions is indicated by the black triangles. Initially (second and third panels), the parent basis functions overlap the ones they spawned yet the subsequent dynamics (lowest panels) are very different: the parent wave function corresponds to an A + BC arrangement and the spawned wave function to an AB + C arrangement. A more detailed, and quantitative, description of the spawning algorithm for both multistate and single state problems can be found in refs 74 and 94, respectively.

The last ingredient required to completely specify the method is the selection of initial conditions (position, momentum, nuclear phase, and electronic amplitude) for the initial basis set. The initial state is modeled as a sum over discrete trajectories sampled from the appropriate Wigner distribution.[95] At this point one has the choice of fitting the trajectory amplitudes such that

$$\langle I|\Psi_{t=0}\rangle = \sum_j C_j^I(t=0)\,\chi_j^I(\mathbf{R};t=0) \quad (2.9)$$

and following all the trajectories simultaneously or assigning unity to each initial amplitude and following the basis functions (i.e., trajectories) one at a time. In the first case, coupled propagation, one attempts a particular form of wave packet propagation with classical mechanics as a guide for basis set selection and propagation. In this mode convergence to exact quantum mechanical results is ensured for a sufficiently large number of basis functions (and in the absence of any approximations, e.g. saddle point). When quantal aspects of the evolution on a single-potential energy surface are important, one should use this option. The second option assumes that a properly chosen swarm of classical trajectories will suffice to describe the dynamics occurring on a single electronic state. In this case, one gives up on the detailed description of interactions between different trajectories representing the initial state and retains only the modeling of inter-trajectory interactions between each initial state trajectory and the trajectories (basis functions) that it spawns. The work described in this article primarily uses the uncoupled representation for the initial state. However, we have used both methods in the past, finding the fully coupled representation to be important in modeling electronic spectra.[96]

The FMS method is computationally more demanding than

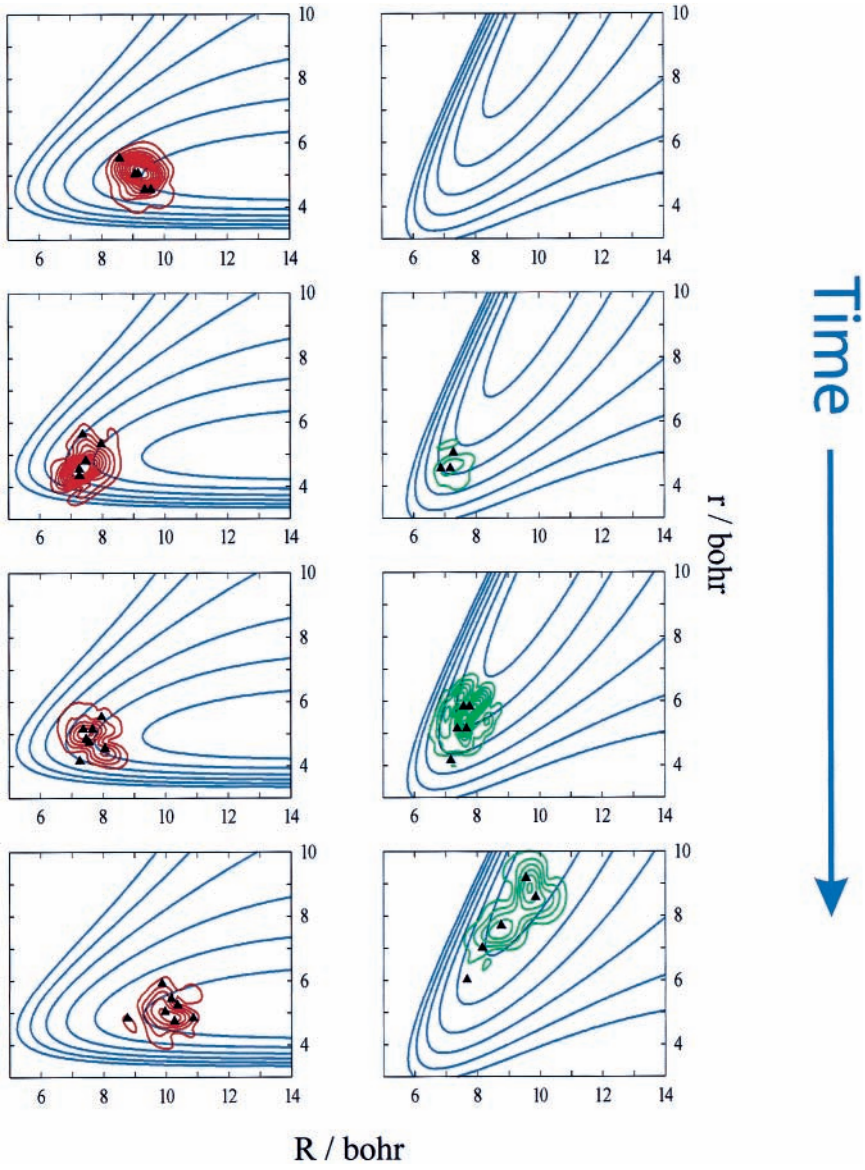

Figure 3. Schematic illustration of the spawning algorithm for a collinear A + BC → AB + C reaction. The right and left panels correspond to two diabatic potential energy surfaces, correlating to A + BC and AB + C, respectively. Blue contour lines denote the potential energy surfaces, represented in Jacobi coordinates (the A to BC center-of-mass distance, *R*, and the BC distance *r*). Superimposed on the contour lines are the nuclear wave functions in the diabatic representation. The calculation begins with population on a single diabatic potential energy surface (uppermost left panel) and as basis functions traverse the nonadiabatic region (atom approaches and then recedes from molecule) new basis functions are created on the other diabatic state (second, third, and fourth right panels). The black triangles indicate the location of individual Gaussian basis functions. Note the initial overlap between the parent basis functions and the ones they spawned, as well as the very different ensuing dynamics: an asymptotic A + BC configuration for the ground state wave function and AB + C for the excited state wave function that it spawned.

other approximate methods designed to model nonadiabatic dynamics for large systems, e.g., surface-hopping procedures,[30,97−101] Pechukas force methods,[102−104] and mean-field approximations.[105−108] A detailed and systematic study comparing all of these methods with FMS has yet to be performed. However, a few general comments can be made from analytic considerations and comparisons in low-dimensional model problems.[72,74] The FMS method automatically conserves wave function normalization. This is absolutely necessary when computing branching ratios for a nonadiabatic process, and is a property shared by surface-hopping and mean-field approaches. In contrast, the Pechukas[102] force method as implemented in ref 103 does not conserve normalization automatically. Furthermore FMS is not stochastic with respect to the nonadiabatic event. The "fewest-switches" surface-hopping scheme of Tully[99] requires double averaging of trajectories (the first is the usual ensemble average over initial conditions and the second is over the subset of trajectories that undergoes a nonadiabatic event). This could imply that many trajectories will be required to compute stable branching ratios (a disastrous implication for an AIMD method). For a set of one-dimensional problems proposed by Tully,[99] we have indeed shown[109] that convergence of branching ratios is much faster with the FMS method than with surface hopping. Using a two-dimensional model problem,[74] we have also demonstrated that the FMS method is able to correctly predict branching ratios at low energies where surface-hopping methods fail due to their inability to consistently account for (classically) energetically forbidden hopping attempts. Because of their simplicity and ease of numerical implementation, mean-field related approximations are attractive. However, their range of applicability is still in question. These methods assume that an ensemble of independent trajectories traveling on a time-dependent average of the PESs is sufficient to describe the dynamics. As has been

previously discussed by Tully,[99,110] one expects these methods to fail when the different electronic states are of different character, e.g., one is bound and the other is dissociative. However, it has also been shown that when the motion is strongly diabatic, as is sometimes found at conical intersections, the dynamics may be qualitatively correct.[111−113]

3. Scaling and Numerical Considerations. Because of the locality of quantum chemistry, a traveling localized nuclear basis set is ideally suited to AIMS. Furthermore, it can be pushed to convergence for problems with few degrees of freedom. This has been explicitly demonstrated for time-dependent electronic populations.[74] There are however disadvantages. Demonstrating convergence for problems with many degrees of freedom is difficult and often impossible, especially when the PES is so expensive that one must be satisfied with few trajectories.

Although in principle it would be desirable to study the numerical convergence and scaling of the FMS method in the context of AIMS, this is not computationally feasible. As a consequence, our comparisons to quantum mechanically converged results have been confined to low-dimensional models with analytic PESs. A few general conclusions can be drawn from these studies. Foremost, one has to distinguish between single surface convergence and convergence of the quantum mechanics associated with the nonadiabatic event. Convergence of the latter, which is dominated by the number of spawned basis functions, does not necessarily imply convergence of the former, which depends on the number of initial nuclear basis functions. To some extent, these two criteria are intertwined. If the accuracy of the wave packet when it enters the nonadiabatic region is poor, so too will be the subsequent nonadiabatic dynamics, regardless of the number of basis functions that are spawned. Since for multistate problems we do not allow for spawning on the same electronic state, the initial size of the basis determines the accuracy of the propagation from the asymptotic region (e.g., the Franck−Condon region) into the nonadiabatic coupling region. For a given initial basis set, the shorter this propagation time, the better the quality of the wave packet in the nonadiabatic region. Since photodynamics is often characterized by short time scales, this is an ideal area for application of AIMS from the standpoint of accuracy as well as computational feasibility.

Formally, scaling is also exponential in the number of degrees of freedom. Here again, one should be careful to distinguish between scaling with respect to single-surface quantum mechanics and scaling with respect to the quantum mechanics of nonadiabatic events. The tests that would be required to say anything definitive about the practical scaling in the former case have yet to be carried out. However, we can say that the scaling in the latter case is definitely not exponential. Empirically, this is evidenced by the fact that between three and five spawned basis functions per nonadiabatic event is usually enough to obtain convergence in the population transfer, independent of the number of molecular degrees of freedom. Physically, it arises because the spawned basis functions are related to a single classical-like trajectory that is a quasi-one-dimensional object, independent of the number of atoms in the molecule.

Having said all of this, we would like to comment on the correlation between the quality of the propagator and that of the results, e.g., expectation values. Our experience,[94] and that of others,[114,115] suggests that expectation values converge long before the wave function. The simplest example that supports this empirical observation is a free particle. When a localized basis of fixed size is used, spreading makes the wave function deteriorate. Yet expectation values may be well predicted. Although the wave function is far from converged, the average position and even the second moment of the wave function can be correctly predicted. Indeed, classical mechanics of the Wigner distribution already does a good job in this regard.[116] It might therefore be prudent to change the focus of inquiries concerning scaling from the accuracy of the time-evolving wave function to the accuracy of the relevant (possibly projected) expectation values. A similar redefinition of this question occurred early on in quantum chemistry, when it was recognized that appropriately designed methods could obtain much higher accuracy in the computation of chemically relevant energy differences than was feasible for the absolute energies of reactants and products.

III. Applications

1. Photoinduced cis−trans Isomerization of Ethylene. In both chemical and biochemical systems the conversion of light energy to mechanical energy is often achieved via photoinduced cis−trans isomerization in unsaturated systems. Typical examples that have attracted much theoretical and experimental attention include the photochemistry of stilbene,[117] the primary event in vision,[118] and cis−trans isomerization of retinal protonated Schiff base in bacteriorhodopsin.[119] Theoretically, unsaturated alkenes pose a challenge to quantum chemistry because the description of their lowest excited electronic states requires a careful treatment of electron correlation. For example, the ordering of the lowest lying doubly excited A_g and singly excited B_u states is very sensitive to the details of the wave function used, and this ordering has been the source of a long controversy in the case of butadiene.[120] Given the many theoretical and experimental studies and the importance of polyene photochemistry in biological systems and molecular switching devices, our incomplete understanding of the photoisomerization mechanism is quite surprising.

The simplest unsaturated hydrocarbon, ethylene, provides a paradigm for the photochemistry of alkenes. However, it should be realized from the outset that it is also special in some respects. Simple particle in a box considerations suggest (and theory and experiment confirm) that as the size of the conjugated system decreases its excitation energy increases. Hence, ethylene has a large excitation energy but at the same time it also has a small number of internal modes. Consequently, it is not surprising that photoexcitation of ethylene leads to fragmentation in addition to the photoisomerization that is the hallmark for larger polyenes.[121−123] This added complexity is accompanied by unresolved issues regarding the absorption and resonance Raman spectrum of ethylene, which are partially due to incomplete knowledge of the character of the manifold of excited electronic states. The following crude statements about the singly excited state of ethylene can be made. Upon absorption of a photon by ethylene, an electron is promoted from a bonding π molecular orbital (MO) to an antibonding π^* MO. While the ground electronic state is planar and stable with respect to twisting, the excited state favors a twisted D_{2d} geometry to minimize both the kinetic energy associated with the antibonding π^* orbital and the Coulomb repulsion between the p electrons of the two carbon atoms. Hence, the electronic excitation results in geometric relaxation toward a stretched (formally the bond order is reduced from 2 to 1) and twisted geometry. Both the interpretation and the controversy regarding the absorption and resonance Raman spectrum of ethylene are based on these considerations.

The absorption spectrum of ethylene exhibits a broad diffuse band that has been assigned by Wilkinson and Mulliken[124] to

the $\pi \rightarrow \pi^*$ valence (V) and Rydberg (R) states. Originally the single progression in the V state band of ethylene was assigned, based on an isoelectronic analogy between O_2 and C_2H_4, to the C=C stretching motion.[124] This assignment was questioned by later investigators, who suggested a purely torsional progression.[125] Subsequently, based on their spectral study of ethylene isotopomers, Foo and Innes[126] agreed with the reassignment, but suggested a mixture of C=C stretching and torsion. When theoretical investigations[51] predicted that the change in the C=C bond length on the excited (V) state was less than 0.1 Å, Mulliken became convinced that the torsion dominated the spectrum.[127,128] Siebrand and co-workers[129] challenged the accepted assignment of mixed torsion and stretching by presenting theoretical evidence that there is no visible stretching activity in the spectrum. Consequently, there have been few challenges to the torsional assignment of the progression, but recently, the very identity of the bands has been questioned.[130] These uncertainties regarding the excited state motion were exacerbated when the possible role of a third coordinate—pyramidalization—was suggested.

The pyramidalization coordinate of ethylene has first been studied in the context of the concept of "sudden polarization."[131−133] There are two low-lying valence excited states of ethylene—the V (covalent) and Z (ionic) states in Mulliken's notation. As first noted by Salem and co-workers,[131,132] and subsequently by Brooks and Schaefer,[133] pyramidalization of twisted ethylene, keeping the molecule in C_s symmetry, results in a large dipole moment. The onset of this phenomenon is quite sudden; i.e., small distortions result in a large change in the dipole moment (which is identically zero at a twisted geometry). This arises because of an avoided crossing between the V and Z states very near the twisted, nonpyramidalized geometry. Whereas the importance and implications of sudden polarization have been questioned, both theory and experiment suggest that the pyramidalization coordinate does participate in the excited state dynamics. The theoretical evidence is based on restricted geometry optimizations of the excited electronic state of ethylene.[133,134] These optimizations have found that the lowest excited state has a minimum at a nonsymmetrical pyramidalized geometry. Resonance Raman studies find overtone activity in both out-of-plane wagging and rocking vibrations,[135] supporting a role for pyramidalization in the initial motion of ethylene after photoexcitation.

The absence of fluorescence after photoexcitation of ethylene suggests a short excited state lifetime. This also holds for butadiene and hexatriene, but not for the larger polyenes where fluorescence is observed. There have been a number of ultrafast pump−probe experiments[136,137] aimed at studying the excited state dynamics of hexatriene (in solution) which have established an upper bound of 500 fs for the excited state lifetime. An obstacle to the analogous experiments for ethylene has been the difficulty of obtaining femtosecond pulses in the deep ultraviolet. This obstacle is now being overcome, and the first femtosecond pump−probe investigation of ethylene has been reported.[138] The AIMS results are compared directly to this experiment below.

Given the above experimental summary, one can anticipate that the photodynamics of ethylene will occur on a subpicosecond time scale, and that it will involve twisting. To some extent stretching and pyramidalization may also be involved, although this will be more controversial. We have carried out AIMS simulations of the photodynamics upon $\pi \rightarrow \pi^*$ excitation. In the following, we limit our discussion to the photochemical mechanism of cis−trans isomerization, but we note

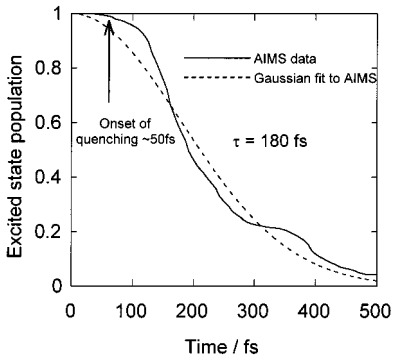

Figure 4. Excited state population of ethylene as a function of time in femtoseconds (full line). The results are averaged over 10 calculations. Quenching to the ground electronic state begins ~50 fs after the electronic excitation, and a Gaussian fit to the AIMS data (dashed line) predicts an excited state lifetime of 180 fs.

that we have also recently used AIMS to compute the electronic absorption and resonance Raman spectra.[96] Furthermore, we do not discuss the photofragmentation dynamics except to note that the AIMS simulations do predict extensive fragmentation on the ground electronic state that is only partially completed within 1 ps.

The AIMS simulations treat the excitation as being instantaneous and centered at the absorption maximum. Thus, the initial state nuclear basis functions are sampled from the Wigner distribution for the ground state molecule in the harmonic approximation. A single initial basis function is used in each simulation, and the results of 10 such simulations are averaged. Each simulation is followed for 500 fs and leads to approximately 10 spawned nuclear basis functions. The results for the excited state lifetime are presented in Figure 4, where both the raw data and a Gaussian fit are shown. A time constant of 180 fs can be inferred, in general agreement with the expectation of subpicosecond dynamics. The decay is clearly nonexponential, which might be expected from time-reversibility arguments given the femtosecond time scales that are involved. Furthermore, one should note that the excited state population does not begin to decay appreciably until approximately 50 fs has elapsed after the optical excitation. This behavior is consistent with the expectation that a conical intersection must be accessed for excited state quenching, requiring some minimal amount of nuclear motion.

A more detailed account of the excited state dynamics is given in Figure 5, where we show several snapshots of the centroid of the dominant nuclear basis function, along with a rendition of the two active orbitals comprising the electronic wave function. Concentrating first on the behavior of the nuclei, one sees that the molecule begins in the expected planar geometry. After 50 fs, the molecule is clearly twisted as expected. However, recall that excited state quenching does not even begin until 50 fs. Thus, torsion is not the sole coordinate responsible for the return to the ground electronic state. Indeed, this can be inferred from the PESs in Figure 1, where the gap between the ground and excited electronic states is large at the twisted D_{2d} geometry ($\approx$3 eV). After 110 fs, one of the methylene units becomes pyramidalized, and it is at this point that quenching to the ground state becomes significant. Further snapshots show attempts at hydrogen migration (200 and 280 fs), which in this example are not successful.

We turn now to the electronic structure during the dynamics. Superimposed on each of the molecular geometries is an isosurface rendition of the two natural orbitals in the CI wave function corresponding most closely to π and π^* orbitals. The

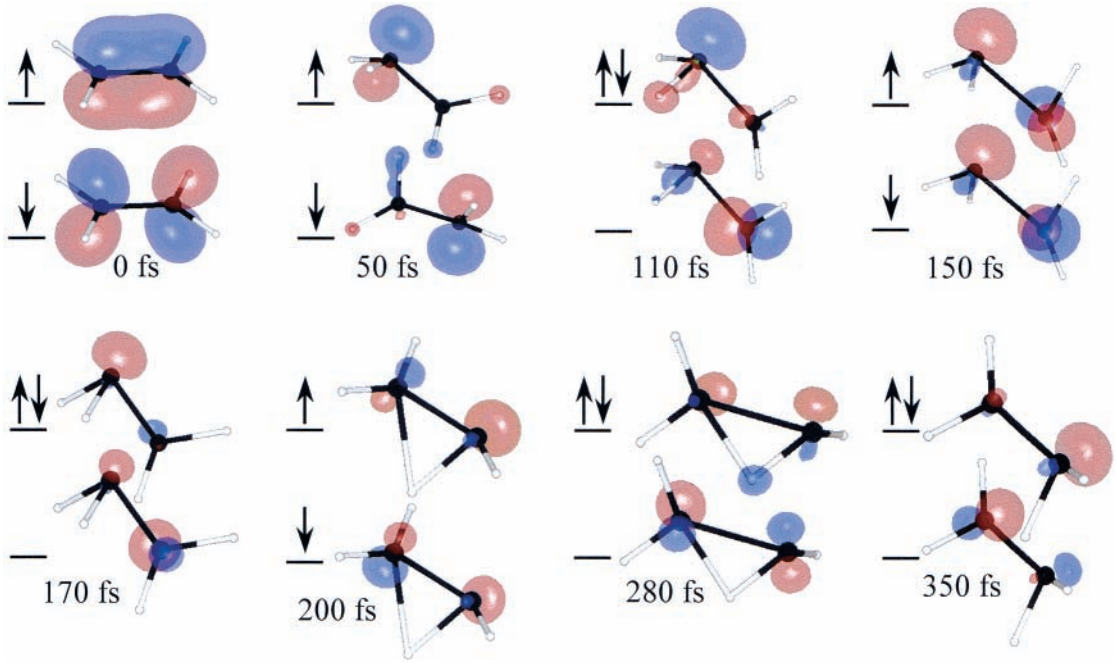

Figure 5. Snapshots of the π- and π^*-like natural orbitals (computed from the OA-GVB-CAS(2/2)*S wave function) of an individual nuclear basis function traveling on the excited electronic state of ethylene. The occupation of each orbital is indicated by the arrows drawn on the energy levels to the left of the orbital. The calculation begins at a planar geometry where the excited state wave function has covalent ($\pi \rightarrow \pi^*$) character. During the course of the dynamics, the excited state wave function oscillates between covalent (50, 150, and 200 fs) and ionic (110, 170, 280, and 350 fs) forms. Attempts at hydrogen migration are observed for both ionic and covalent wave functions (snapshots at 200 and 280 fs).

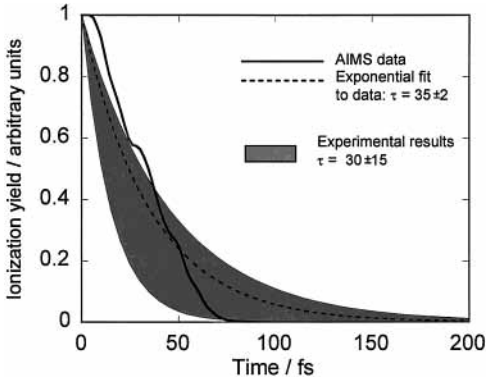

Figure 6. C_2H_4 ion yield as a function of time in femtoseconds. Heavy line: predicted ion yield using AIMS data and assuming an ionization threshold of 3.5 eV. Dashed line: predicted ion yield using an exponential fit to the AIMS data with an excited state lifetime of 35 ± 2 fs and assuming an ionization threshold of 3.5 eV. Gray shaded area: the reported ion yield[138] obtained using an exponential fit to the experimental data with an excited-state lifetime of 30 ± 15 fs.

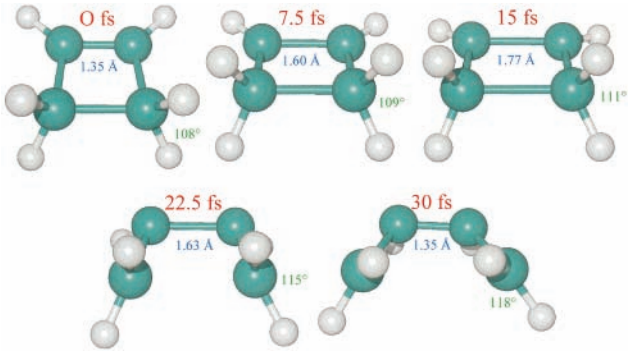

Figure 7. Snapshots of a typical excited state trajectory of cyclobutene. The values of the CC double bond distance and the HCH hybridization angle are indicated. Following the electronic excitation the first motion is a stretching of the CC double bond. This is followed by a change in hybridization of the methylene carbons and by a pronounced disrotatory motion.

occupation of these orbitals (rounded to the nearest integer) is denoted by the arrows in the energy level diagram to the left of each snapshot. The expected π and π^* orbitals are evident at 0 fs, immediately after the $\pi \rightarrow \pi^*$ excitation. Already at 50 fs, breakdown of $\sigma-\pi$ separation is observed, as evidenced by the significant contribution of 1s character from the H atoms. Although the decreased symmetry on the excited state makes this breakdown expected, it is perhaps surprising that it happens so quickly. At 110 fs, the excited electronic state is best described as a double excitation, with both electrons localized on one of the methylene units. This is accompanied by considerable pyramidalization of the anionic carbon atom, suggesting that the molecule is now on the Z electronic state. However, at 150 fs, the electronic state is again well-described as a single excitation; i.e., the molecule is on the V state. The situation changes again at 170 fs. Thus, one can characterize the excited state dynamics as consisting of electron transfer between the two methylene units. This can be understood from the PES in Figure 1, where it is clear that the D_{2d} twisted geometry is a saddle point connecting two minima on the excited state PES (where alternately the left and right methylene units are pyramidalized). The intramolecular electron transfer dynamics is punctuated by quenching to the ground state each time the molecule reaches one of the excited state minima, since these are in close proximity to a conical intersection (see Figure 1). Hence, the AIMS results paint a picture of the ethylene photochemistry that intimately involves the pyramidalization *and* torsional motions, and where the excited state dynamics involves *both* the V and Z states. This picture can be contrasted with the above discussion of experimental results, which centered on the torsional coordinate and the role of the V state.

Although the experimental information does support the qualitative picture that comes from the AIMS simulations, a direct comparison would be desirable. The recent experiment

of Radloff and co-workers[138] provides the short-time information that is ideal for this purpose. The experiment is of the pump−probe variety, with ionization induced by the probe pulse. Assuming an exponential decay of the ionizable excited state, Radloff and co-workers obtained a lifetime of 30 ± 15 fs. If the AIMS data is correct, this is much too short to be considered as an excited state lifetime, and the possibility of a dark form of the excited state should be entertained. Direct simulation of this experiment has been carried out using the AIMS data, assuming that molecules ionize with 100% efficiency provided the excited state ionization potential is below the threshold given by the probe pulse. The results are shown in Figure 6, along with an exponential fit. The time constant obtained by the exponential fit (35 ± 2 fs) lies comfortably within the experimental error bars (the range consistent with the experimental results is shown by the shaded area). This agreement is encouraging and provides support for the veracity of our results. It also suggests that the experiment is probing the excited state only within a limited window around the Franck−Condon region, thus providing a lower bound on the excited state lifetime. In this picture, most of the excited state dynamics, after significant twisting which is discussed above and shown in caricature in Figure 5, is invisible to the experiment. A further caution comes from the fact that the AIMS results are clearly poorly modeled by an exponential decay. It may not be fruitful to analyze this much further at present since the time resolution of the experimental pump and probe pulses is only 125 fs. However, it is possible to perform a more complete AIMS modeling of the experiment, explicitly accounting for the finite duration of the laser pulses. This would allow direct comparison of simulated and experimental ion yield signals, without going through the exercise of fitting both sets of data to a possibly inappropriate model.

2. Photochemical Ring Opening of Cyclobutene. The formulation of the Woodward−Hoffmann[139] (WH) and related rules[140−142] represented a monumental advance in our understanding of the relationship between orbital phase and barriers to chemical reactions. While the applicability of the rules is sometimes hotly debated for the thermal reactions,[143] i.e., whether the reactions are concerted or sequential, the success of the rules is undeniable in these cases. Furthermore, it is quite clear that, at least when the reaction in question is concerted, the rules give the right answer for the right reason. The treatise of Woodward and Hoffmann remains an excellent explication of the rules, but the reader is also referred to several recent articles that have provided a detailed analysis of the subtleties of the rules in light of modern-day electronic structure theory.[144,145]

Such a happy state of affairs does not obtain for the photochemical variants of the rules. Particularly in the case of ring-opening reactions for substituted cyclobutenes, there are many cases where the WH-predicted stereochemistry is not obtained in the photoproducts.[146] Furthermore, it has been established that the electronic state that is relevant in orbital symmetry conservation principles is populated for as little as 50 fs, whereupon nonadiabatic transitions to a second excited electronic state (about which the WH rules are silent) occur.[147,148] Despite this fact, the WH-predicted stereochemistry is observed in certain alkyl-substituted cyclobutene ring openings.[149] The situation is thus rather murky. The rules are not obeyed for many cases, and even when they are obeyed, a WH state is apparently only populated for a few molecular vibrations. The first important question that must be answered is how long it takes for motion along the WH-predicted coordinate to develop. Should this time be comparable to the excited state lifetime, one might conclude that the photochemical and thermal rules work for the same reason—the relative barrier heights for different motions (disrotatory vs conrotatory in the case of ring-opening reactions) are determined by orbital symmetry/phase considerations. On the other hand, if this time is very short, one might instead conclude that the thermal and photochemical rules have very different character, with the photochemical rules originating from an impulsive approximation to the excited state dynamics.

Mathies and co-workers have used time-resolved resonance Raman experiments to investigate this situation for a number of ring-opening reactions, including that of cyclobutene.[147] Intensity was observed in an overtone of the 1075 cm^{-1} (ν_{15}) normal mode at 2150 cm^{-1}, implying that the corresponding motion plays a significant role in the excited state dynamics on a time scale shorter than that of the resonance Raman experiment (≈50 fs). Earlier work[150,151] indicated that the ν_{15} normal mode (b_1 symmetry) is of disrotatory character. (Note that the disrotatory and conrotatory modes are not normal modes.) Relying on this assignment, Mathies concluded that the WH-predicted disrotatory motion is established early in the photochemistry. Later workers[152] presented theoretical evidence that a conflicting assignment[153] due to Wiberg et al. was correct. According to this assignment, the overtone Mathies observed corresponds to a CH_2 wagging motion, also of b_1 symmetry, not a disrotatory ring opening. The normal mode that this assignment predicts to correspond to disrotatory motion, ν_{16}, has a frequency of 848 cm^{-1}, and thus the lowest overtone is expected at 1696 cm^{-1}. Unfortunately, this region of the spectrum is dominated by scattering from butadiene photoproduct, precluding a straightforward reinterpretation of the experimental data. Although a femtosecond pump−probe experiment might be possible that could settle the issue, little more has been said about it. Thus, we have used the AIMS method to investigate the ultrafast excited state dynamics of cyclobutene immediately following photoexcitation.

The electronic structure is treated in a fashion similar to that of ethylene, using a HF-OA-CAS(4/4)*S wave function where the four active orbitals are those which become the two π orbitals in the butadiene photoproduct. Initial conditions for the classical trajectory basis functions after photoexcitation are chosen from the Wigner distribution corresponding to the ground state (vibrational and electronic) cyclobutene molecule in the normal mode approximation. The trajectory basis functions are not coupled, and only the short-time dynamics has been investigated (up to 50 fs). Four distinct initial conditions are employed. For this short propagation time and small set of initial conditions, we did not observe any nonadiabatic effects.

We find that motion along the disrotatory, i.e., WH-allowed, coordinate is immediate, thus confirming Mathies' conclusion (but, as discussed below, only partially confirming the experimental interpretation). This is an important result because it establishes that the WH rules are at least in part based on an implicit impulsive approximation in the excited state manifold. In Figure 7, we show snapshots of a single trajectory basis motion after photoexcitation. All other basis functions behave similarly. The first motion is a stretching of the CC double bond, whose formal bond order is reduced from 2 to 1. Shortly thereafter, the hybridization of the methylenic carbon atoms changes from sp^2 to sp^3. Finally, and within 20 fs of the photoexcitation, significant displacement along the disrotatory coordinate occurs. This is quite clearly discernible in Figure 7, but a quantification of the results is also desired. This is shown in Figure 8, where the expectation values of the hybridization

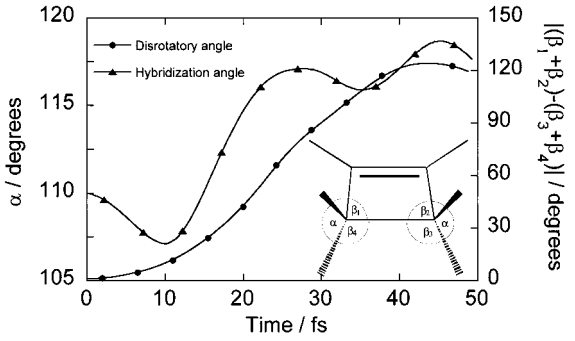

Figure 8. The disrotatory angle (full line with circles and right *y* axis) and the HCH hybridization angle (full line with triangles and left *y* axis) as a function of time in femtoseconds. Results are averaged over four trajectories traveling on the first excited electronic state of cyclobutene. The absolute value of the disrotatory angle is defined as $|(\beta_1 + \beta_2) - (\beta_3 + \beta_4)|$. (See inset for definition of the β and α angles.) The change in hybridization (from sp^3 to sp^2) begins almost immediately after the electronic excitation and is completed within 50 fs. The disrotatory motion begins approximately 10 fs after the electronic excitation and its amplitude is large (120°).

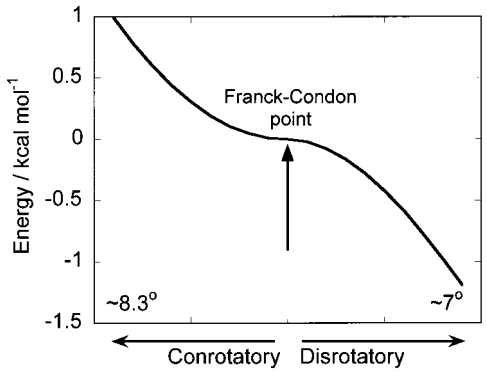

Figure 9. One-dimensional cut of the excited state potential energy surface of cyclobutene along the disrotatory and conrotatory coordinates. All other coordinates are kept at their ground state equilibrium value. Along the disrotatory coordinate the excited state potential is attractive, and it is repulsive along the conrotatory coordinate.

and disrotatory angles for the entire set of trajectory basis functions are shown. In this figure, the disrotatory angle is defined not in terms of ground state normal modes, but rather in terms of local modes in symmetry-adapted internal coordinates. We use Wiberg's definition of the disrotatory angle,[153] given in the inset of the figure. Notice the range of the disrotatory angle over the 50 fs time scale shown—it increases from 0° to 120°. The rationale for this behavior must certainly be found in the excited state potential energy surface. Thus, it is instructive to examine the excited state potential energy surface for displacements along the disrotatory and conrotatory modes. Both of these modes are nontotally symmetric and therefore the ground state equilibrium value must be a stationary point on the excited state. Indeed, this is the case, but the important point is that on the excited state and at the ground state equilibrium value, the disrotatory coordinate has a saddle point, while the conrotatory coordinate has a minimum. This is shown in Figure 9, where the Franck−Condon point is at the midpoint of the *x* axis, and the disrotatory coordinate extends to the right while the conrotatory coordinate extends to the left (the excited state PES in both cases is symmetric with respect to reflection about the Franck−Condon point). All other normal modes are left at their Franck−Condon values in this plot. The expected dynamics is clear. The wave packet produced on the excited state will remain bound in the conrotatory (WH-forbidden) coordinate and will evolve along the disrotatory (WH-allowed) coordinate. The only impediment to immediate motion along the disrotatory coordinate is the fact that the Franck−Condon point is a saddle point. Thus, for example, a purely classical trajectory with geometry corresponding to the equilibrium ground state without any zero-point energy would remain on the ridge forever. Quantum mechanical effects are expected to minimize the relevance of such a classical periodic orbit. Thus evolution along the disrotatory coordinate should be essentially immediate (as we observe in the AIMS calculations).

We have analyzed the character of the normal modes and must agree with Negri and co-workers[152] that the assignment[150,151] on which Mathies[147] based his interpretation is incorrect. Although there is some component of disrotatory motion in the 1075 cm^{-1} normal mode, the mode is dominantly a CH_2 wag. Nevertheless, by following the excited state dynamics we can conclude that the WH tendency is established during the first femtoseconds of the ring opening. This suggests a role for impulsive character and kinematic effects on the efficacy of the WH rules for photochemical reactions. Indeed, one might then expect that classification of the cyclobutene and substituted cyclobutene ring-opening reactions which do and do not lead to the WH-predicted stereochemistry could be correlated with the effective mass of the substitutents—the heavier the substitutents, the more likely that the initial WH-directed impulse could be overcome by the detailed landscape of the excited state potential energy surface. Further calculations and experiments, for example using deuterated cyclobutene, are needed to make progress in formulating such a theory.

IV. Outlook and Conclusions

The work presented in this paper shows that it is possible to model photochemical reaction dynamics from first principles for molecules of general chemical interest. However, there remain many directions for improvement. The electronic structure treatment that we have used does not do full justice to the Rydberg states of the molecule. Yet, it is well-established that in the Franck−Condon region, the lowest-lying excited states of at least the smaller unsaturated hydrocarbons are Rydberg states. Compared to the higher-lying, optically accessible valence excited states, the energies of the Rydberg states are relatively insensitive to molecular geometry. Thus, one expects (and finds theoretically) that as the geometry of the molecule varies to minimize the valence excited state energy, a series of avoided crossings and/or intersections with Rydberg states will be encountered. Furthermore, there will generally be some amount of Rydberg−valence mixing in the Franck−Condon region that will however decrease as the geometry of the molecule changes to favor the valence excited state. One can conclude that a "de-Rydbergization" process must occur as the molecule finds its way from the Franck−Condon region to the ground state. This de-Rydbergization process is poorly understood, and is not addressed in the present work. Effectively, our calculations assume that de-Rydbergization is immediate and that henceforth the Rydberg states are spectator states; i.e., the dominant evolution is diabatic with respect to the valence/Rydberg character of the excited state. Certainly this is an approximation that must be less successful at some levels than others. For example, the character of the electronic absorption spectrum would be expected to be more sensitive to this issue. Indeed, a Rydberg state has recently been proposed to play a dominant role in the absorption spectrum of ethylene.[130] We are currently exploring the role of the Rydberg states by carrying

out calculations on ethylene with more extended basis sets, but it must be admitted that these calculations are extremely demanding of computational resources and border on what is practically possible with the present methodology. Certainly, such studies on cyclobutene and butadiene, while of great interest to us, are not yet possible. While the ever-increasing speed of computers will likely make these possible soon, there is a clear need for new approaches to the electronic structure of excited states. Time-dependent density functional theory is one promising avenue.[38,40,154] Others include hybrid molecular orbital/valence bond theory approaches,[89,155] combinations of interpolation and direct dynamics strategies,[156,157] and hybrid quantum mechanical/classical electrostatic models of potential energy surfaces.[158−160]

Similarly, improvement in the accuracy of the nuclear dynamics would be fruitful. While it has been shown that the FMS treatment of the nuclear dynamics can border on numerically exact for systems with a couple of degrees of freedom, we certainly do not claim this for the applications presented here. Due in part to a paucity of models with many degrees of freedom where the quantum dynamics is exactly soluble, we do not have a firm prescription for assessing the accuracy of the FMS approximations in large molecules. In principle, we can carry out sequences of calculations with larger and larger nuclear basis sets in order to demonstrate that interesting experimentally observable quantities have converged. In the context of AIMS, the cost of the electronic structure calculations precludes systematic studies of this convergence behavior for molecules with more than a few atoms. It is interesting to note that a similar situation obtains in time-independent quantum chemistry—the only reliable way to determine the accuracy of a particular calculation is to perform a sequence of calculations in a hierarchy of increasing basis sets and electron correlation. What is critically different about time-independent quantum chemistry is that well-defined and extensively tested hierarchies exist, e.g., the correlation consistent basis sets of Dunning and co-workers[58,161,162] and the increasing orders of perturbation theory, MP*n*.[163] Developing such hierarchies for the FMS method is an important goal that is prerequisite to the widespread use of AIMS. We are working toward this goal, but it is important to recognize that it will only be useful if it arises from an extensive set of applications. It is not fruitful to propose a computational hierarchy unless the incremental improvements going from one step to the next are similar throughout, and at the present stage it appears that this can only be determined empirically.

Finally, there are new directions that should be pursued. The AIMS approach emphasizes a particular type of quantum mechanical effect in the nuclear dynamics—nonadiabatic transitions. Yet, other quantum mechanical effects can be important to chemistry, notably zero-point energy and tunneling. Because the FMS dynamics used in AIMS may be considered a form of basis set expansion solution to the nuclear Schrödinger equation, these effects have not been arbitrarily removed. However, there is no question that the AIMS method does not focus on an accurate treatment here—the adaptive nature of the basis set does not take these effects into account. We have recently proposed[94] an extension of the AIMS method that incorporates tunneling effects by spawning "on the other side of the barrier." Similar extensions to the concept of spawning can be envisioned which allow nuclear dispersion effects to be accurately treated. However, it is not clear that this would be computationally practical—to be useful it must be possible to aggressively limit the rate of basis set expansion. The temporal localization in nonadiabatic and tunneling events (given a localized nuclear wave packet) provides a means to limit this expansion, but spreading effects cannot obviously be so effectively localized.

Acknowledgment. We thank Prof. E. R. Davidson for a careful reading of the manuscript prior to publication. This work has been supported by the U.S. Department of Energy through the University of California under Subcontract No. B341494, the National Science Foundation (CHE-97-33403), and the National Institutes of Health (PHS-5-P41-RR05969). T.J.M. is the grateful recipient of CAREER, Research Innovation, Beckman Young Investigator, and Packard Fellow awards from NSF, Research Corporation, The Beckman Foundation, and The Packard Foundation, respectively.

References and Notes

(1) Pulay, P. *Mol. Phys.* **1969**, *17*, 197.
(2) Yamaguchi, Y.; Osamura, Y.; Goddard, J. D.; Schaefer, H. F. *A New Dimension to Quantum Chemistry: Analytic Derivative Methods in Ab Initio Electronic Structure Theory*; Oxford University Press: Oxford, 1994.
(3) Ishida, K.; Morokuma, K.; Komornicki, A. *J. Chem. Phys.* **1977**, *66*, 2153.
(4) Fukui, K.; Kato, S.; Fujimoto, H. *J. Am. Chem. Soc.* **1975**, *97*, 1.
(5) Fukui, K. *J. Phys. Chem.* **1970**, *74*, 4161.
(6) Miller, W. H.; Handy, N. C.; Adams, J. E. *J. Chem. Phys.* **1980**, *72*, 99.
(7) Gray, S. K.; Miller, W. H.; Yamaguchi, Y.; Schaefer, H. F. *J. Chem. Phys.* **1980**, *73*, 2733.
(8) Colwell, S. M.; Handy, N. C. *J. Chem. Phys.* **1985**, *82*, 1281.
(9) Baldridge, K. K.; Gordon, M. S.; Steckler, R.; Truhlar, D. G. *J. Phys. Chem.* **1989**, *93*, 5107.
(10) Truong, T. N. *J. Chem. Phys.* **1994**, *100*, 8014.
(11) Maierle, C. S.; Schatz, G. C.; Gordon, M. S.; McCabe, P.; Connor, J. N. L. *J. Chem. Soc., Faraday Trans.* **1997**, *93*, 709.
(12) Allison, T. C.; Lynch, G. C.; Truhlar, D. G.; Gordon, M. S. *J. Phys. Chem.* **1996**, *100*, 13575.
(13) Weakliem, P. C.; Wu, C. J.; Carter, E. A. *Phys. Rev. Lett.* **1992**, *69*, 200.
(14) Desainteclaire, P.; Barbarat, P.; Hase, W. L. *J. Chem. Phys.* **1994**, *101*, 2476.
(15) Guallar, V.; Batista, V. S.; Miller, W. H. *J. Chem. Phys.* **1999**, *110*, 9922.
(16) Leforestier, C. *J. Chem. Phys.* **1978**, *68*, 4406.
(17) Car, R.; Parrinello, M. *Phys. Rev. Lett.* **1985**, *55*, 2471.
(18) Hartke, B.; Carter, E. A. *Chem. Phys. Lett.* **1992**, *189*, 358.
(19) Hartke, B.; Carter, E. A. *J. Chem. Phys.* **1992**, *97*, 6569.
(20) Fantucci, P.; Bonacic-Koutecky, V.; Jellinek, J.; Wiechert, M.; Harrison, R. J.; Guest, M. F. *Chem. Phys. Lett.* **1996**, *250*, 47.
(21) Jellinek, J.; Bonacic-Koutecky, V.; Fantucci, P.; Wiechert, M. *J. Chem. Phys.* **1994**, *101*, 10092.
(22) Maluendes, S. A.; Dupuis, M. *Int. J. Quantum Chem.* **1992**, *42*, 1327.
(23) Hammes-Schiffer, S.; Andersen, H. C. *J. Chem. Phys.* **1993**, *99*, 523.
(24) Parrinello, M. *Solid State Commun.* **1997**, *102*, 107.
(25) Gordon, M. S.; Chaban, G.; Taketsugu, T. *J. Phys. Chem.* **1996**, *100*, 11512.
(26) Bolton, K.; Schlegel, H. B.; Hase, W. L.; Song, K. Y. *Phys. Chem. Chem. Phys.* **1999**, *1*, 999.
(27) Tuckerman, M. E.; Ungar, P. J.; Vonrosenvinge, T.; Klein, M. L. *J. Phys. Chem.* **1996**, *100*, 12878.
(28) Stich, I.; Gale, J. D.; Terakura, K.; Payne, M. C. *Chem. Phys. Lett.* **1998**, *283*, 402.
(29) Pavese, M.; Berard, D. R.; Voth, G. A. *Chem. Phys. Lett.* **1999**, *300*, 93.
(30) Vreven, T.; Bernardi, F.; Garavelli, M.; Olivucci, M.; Robb, M. A. *J. Am. Chem. Soc.* **1997**, *119*, 12687.
(31) Sprik, M.; Ciccotti, G. *J. Chem. Phys.* **1998**, *109*, 7737.
(32) Dasilva, A. J. R.; Radeke, M. R.; Carter, E. A. *Surf. Sci. Lett.* **1997**, *381*, 628.
(33) Curioni, A.; Sprik, M.; Andreoni, W.; Schiffer, H.; Hutter, J.; Parrinello, M. *J. Am. Chem. Soc.* **1997**, *119*, 7218.
(34) Meijer, E. J.; Sprik, M. *J. Am. Chem. Soc.* **1998**, *120*, 6345.
(35) Zewail, A. H. *J. Phys. Chem.* **1996**, *100*, 12701.
(36) Ditchfield, R.; Del Bene, J. E.; Pople, J. A. *J. Am. Chem. Soc.* **1972**, *94*, 703.

(37) Foresman, J. B.; Head-Gordon, M.; Pople, J. A.; Frisch, M. J. *J. Phys. Chem.* **1992**, *96*, 135.
(38) Singh, R.; Deb, B. M. *Phys. Rep.* **1999**, *311*, 47.
(39) Frank, I.; Hutter, J.; Marx, D.; Parrinello, M. *J. Chem. Phys.* **1998**, *108*, 4060.
(40) Yabana, K.; Bertsch, G. F. *Int. J. Quantum Chem.* **1999**, *75*, 55.
(41) Docken, K. K.; Hinze, J. *J. Chem. Phys.* **1972**, *57*, 4928.
(42) Werner, H.-J.; Meyer, W. *J. Chem. Phys.* **1981**, *74*, 5802.
(43) Werner, H. J.; Meyer, W. *J. Chem. Phys.* **1981**, *74*, 5794.
(44) Lengsfield B. H., III; Yarkony, D. R. *Adv. Chem. Phys.* **1992**, *82*, 1.
(45) Schaefer, H. F.; Bender, C. F. *J. Chem. Phys.* **1971**, *55*, 1720.
(46) Hay, P. J.; Dunning, T. H., Jr.; Goddard, W. A., III. *J. Chem. Phys.* **1975**, *62*, 3912.
(47) Davidson, E. R. *J. Phys. Chem.* **1996**, *100*, 6161.
(48) Goddard, W. A., III; Dunning, T. H., Jr.; Hunt, W. J.; Hay, P. J. *Acc. Chem. Res.* **1973**, *6*, 368.
(49) Ben-Nun, M.; Martínez, T. J. *Chem. Phys. Lett.* **1998**, *298*, 57.
(50) Bender, C. F.; Dunning, T. H., Jr.; Schaefer, H. F., III; Goddard, W. A., III; Hunt, W. J. *Chem. Phys. Lett.* **1972**, *15*, 171.
(51) Buenker, R. J.; Peyerimhoff, S. D. *Chem. Phys.* **1976**, *9*, 75.
(52) Brooks, B. R.; Schaefer, H. F. *J. Chem. Phys.* **1978**, *68*, 4839.
(53) Lindh, R.; Roos, B. O. *Int. J. Quantum Chem.* **1989**, *35*, 813.
(54) Serrano-Andres, L.; Merchan, M.; Nebot-Gil, I.; Lindh, R.; Roos, B. O. *J. Chem. Phys.* **1993**, *98*, 3151.
(55) Cave, R. J. *J. Chem. Phys.* **1990**, *92*, 2450.
(56) Muller, T.; Dallos, M.; Lischka, H. *J. Chem. Phys.* **1999**, *110*, 7176.
(57) Werner, H.-J.; Knowles, P. J.; Almlöf, J.; Amos, R. D.; Berning, A.; Cooper, D. L.; Deegan, M. J. O.; Dobbyn, A. J.; Eckert, F.; Elbert, S. T.; Hampel, C.; Lindh, R.; Lloyd, A. W.; Meyer, W.; Nicklass, A.; Peterson, K.; Pitzer, R.; Stone, A. J.; Taylor, P. R.; Mura, M. E.; Pulay, P.; Schütz, M.; Stoll, H.; Thorsteinsson, T. MOLPRO 98.1, 1998.
(58) Kendall, R. A.; Dunning, T. H., Jr.; Harrison, R. J. *J. Chem. Phys.* **1992**, *96*, 6796.
(59) Knowles, P. J.; Werner, H. J. *Chem. Phys. Lett.* **1988**, *145*, 514.
(60) Werner, H. J.; Knowles, P. J. *J. Chem. Phys.* **1988**, *89*, 5803.
(61) Knowles, P. J.; Werner, H. J. *Theor. Chim. Acta* **1992**, *84*, 95.
(62) Krauss, M.; Mielczarek, S. R. *J. Chem. Phys.* **1969**, *51*, 5241.
(63) Wiberg, K. B.; Hadad, C. M.; Foresman, J. B.; Chupka, W. A. *J. Phys. Chem.* **1992**, *96*, 10756.
(64) Ruedenberg, K.; Atchity, G. J. *J. Chem. Phys.* **1993**, *99*, 3799.
(65) Domcke, W.; Woywod, C. *Chem. Phys. Lett.* **1993**, *216*, 362.
(66) Galloy, C.; Lorquet, J. C. *J. Chem. Phys.* **1977**, *67*, 4672.
(67) Cimiraglia, R.; Persico, M.; Tomasi, J. *Chem. Phys.* **1980**, *53*, 357.
(68) Klessinger, M.; Michl, J. *Excited States and Photochemistry of Organic Molecules*; VCH Publishers: New York, 1995.
(69) Yarkony, D. R. *Rev. Mod. Phys.* **1996**, *68*, 985.
(70) Bearpark, M. J.; Bernardi, F.; Clifford, S.; Olivucci, M.; Robb, M. A.; Vreven, T. *J. Phys. Chem. A* **1997**, *101*, 3841.
(71) Kosloff, R. *Annu. Rev. Phys. Chem.* **1994**, *45*, 145.
(72) Martínez, T. J.; Ben-Nun, M.; Levine, R. D. *J. Phys. Chem.* **1996**, *100*, 7884.
(73) Martínez, T. J.; Ben-Nun, M.; Levine, R. D. *J. Phys. Chem. A* **1997**, *101*, 6389.
(74) Ben-Nun, M.; Martínez, T. J. *J. Chem. Phys.* **1998**, *108*, 7244.
(75) Ben-Nun, M.; Martínez, T. J. *J. Chem. Phys.* **1999**, *110*, 4134.
(76) Heller, E. J. *J. Chem. Phys.* **1975**, *62*, 1544.
(77) Heller, E. J. *Acc. Chem. Res.* **1981**, *14*, 368.
(78) Tannor, D. J.; Heller, E. J. *J. Chem. Phys.* **1982**, *77*, 202.
(79) Heller, E. J.; Sundberg, R. L.; Tannor, D. *J. Phys. Chem.* **1982**, *86*, 1822.
(80) Heller, E. J. *J. Chem. Phys.* **1981**, *75*, 2923.
(81) Walton, A. R.; Manolopoulos, D. E. *Chem. Phys. Lett.* **1995**, *244*, 448.
(82) Anderson, S. M.; Park, T. J.; Neuhauser, D. *Phys. Chem. Chem. Phys.* **1999**, *1*, 1343.
(83) Anderson, S. M.; Zink, J. I.; Neuheuser, D. *Chem. Phys. Lett.* **1998**, *291*, 387.
(84) Cardenas, A. E.; Coalson, R. D. *Chem. Phys. Lett.* **1997**, *265*, 71.
(85) Cardenas, A. E.; Krems, R.; Coalson, R. D. *J. Phys. Chem. A* **1999**, *103*, 9469.
(86) Sawada, S.-I.; Metiu, H. *J. Chem. Phys.* **1986**, *84*, 6293.
(87) Sawada, S.-I.; Heather, R.; Jackson, B.; Metiu, H. *J. Chem. Phys.* **1985**, *83*, 3009.
(88) Martínez, T. J.; Levine, R. D. *Chem. Phys. Lett.* **1996**, *259*, 252.
(89) Martínez, T. J.; Levine, R. D. *J. Chem. Phys.* **1996**, *105*, 6334.
(90) Martínez, T. J. *Chem. Phys. Lett.* **1997**, *272*, 139.
(91) Ruedenberg, K. *J. Chem. Phys.* **1951**, *19*, 1433.
(92) Martínez, T. J.; Levine, R. D. *J. Chem. Soc., Faraday Trans.* **1997**, *93*, 940.
(93) Trotter, M. F. *Proc. Am. Math. Soc.* **1959**, *10*, 545.
(94) Ben-Nun, M.; Martínez, T. J. *J. Chem. Phys.* **1999**, *112*, 6113.
(95) Hillery, M.; O'Connell, R. F.; Scully, M. O.; Wigner, E. P. *Phys. Rep.* **1984**, *106*, 121.
(96) Ben-Nun, M.; Martínez, T. J. *J. Phys. Chem.* **1999**, *103*, 10517.
(97) Tully, J. C.; Preston, R. K. *J. Chem. Phys.* **1971**, *55*, 562.
(98) Preston, R. K.; Tully, J. C. *J. Chem. Phys.* **1971**, *54*, 4297.
(99) Tully, J. C. *J. Chem. Phys.* **1990**, *93*, 1061.
(100) Blais, N. C.; Truhlar, D. G. *J. Chem. Phys.* **1983**, *79*, 1334.
(101) Smith, B. R.; Bearpark, M. J.; Robb, M. A.; Bernardi, F.; Olivucci, M. *Chem. Phys. Lett.* **1995**, *242*, 27.
(102) Pechukas, P. *Phys. Rev.* **1969**, *181*, 174.
(103) Webster, F. J.; Rossky, P. J.; Friesner, R. A. *Comput. Phys. Commun.* **1991**, *63*, 494.
(104) Webster, F.; Wang, E. T.; Rossky, P. J.; Friesner, R. A. *J. Phys. Chem.* **1994**, *104*, 4835.
(105) Meyer, H.-D.; Miller, W. H. *J. Phys. Chem.* **1979**, *70*, 3214.
(106) Meyer, H.-D.; Miller, W. H. *J. Chem. Phys.* **1980**, *72*, 2272.
(107) Mavri, J.; Berendsen, H. J. C.; Gunsteren, W. F. V. *J. Phys. Chem.* **1993**, *97*, 13469.
(108) Billing, G. D. *Int. Rev. Phys. Chem.* **1994**, *13*, 309.
(109) Martínez, T. J.; Ben-Nun, M.; Ashkenazi, G. *J. Chem. Phys.* **1996**, *104*, 2847.
(110) Tully, J. C. Nonadiabatic Processes in Molecular Collisions. In *Dynamics of Molecular Collisions Part B*; Miller, W. H., Ed.; Plenum Press: New York, 1976.
(111) Klein, S.; Bearpak, M. J.; Smith, B. R.; Robb, M. A.; Olivucci, M.; Bernardi, F. *Chem. Phys. Lett.* **1998**, *292*, 259.
(112) Stock, G. *J. Chem. Phys.* **1995**, *103*, 1561.
(113) Stock, G. *J. Chem. Phys.* **1995**, *103*, 2888.
(114) McCoy, A. B.; Gerber, R. B.; Ratner, M. A. *J. Chem. Phys.* **1994**, *101*, 1975.
(115) Braun, M.; Metiu, H.; Engel, V. *J. Chem. Phys.* **1998**, *108*, 8983.
(116) Heller, E. J. *J. Chem. Phys.* **1976**, *65*, 1289.
(117) Waldeck, D. H. *Chem. Rev.* **1991**, *91*, 415.
(118) Schoenlein, R. W.; Peteanu, L. A.; Mathies, R. A.; Shank, C. V. *Science* **1991**, *254*, 412.
(119) Mathies, R. A.; Lin, S. W.; Ames, J. B.; Pollard, W. T. *Annu. Rev. Biophys. Biophys. Chem.* **1991**, *20*, 491.
(120) Orlandi, G.; Zerbetto, F.; Zgierski, M. Z. *Chem. Rev.* **1991**, *91*, 867.
(121) Balko, B. A.; Zhang, J.; Lee, Y. T. *J. Phys. Chem.* **1997**, *101*, 6611.
(122) Evleth, E. M.; Sevin, A. *J. Am. Chem. Phys.* **1981**, *103*, 7414.
(123) McNesby, J. R.; Okabe, H. *Adv. Photochem.* **1964**, *3*, 228.
(124) Wilkinson, P. G.; Mulliken, R. S. *J. Chem. Phys.* **1955**, *23*, 1895.
(125) McDiarmid, R.; Charney, E. *J. Chem. Phys.* **1967**, *47*, 1517.
(126) Foo, P. D.; Innes, K. K. *J. Chem. Phys.* **1974**, *60*, 4582.
(127) Mulliken, R. S. *J. Chem. Phys* **1977**, *66*, 2448.
(128) Merer, A. J.; Mulliken, R. S. *Chem. Rev.* **1969**, *69*, 639.
(129) Siebrand, W.; Zerbetto, F.; Zgierski, M. Z. *Chem. Phys. Lett.* **1990**, *174*, 119.
(130) Ryu, J.; Hudson, B. S. *Chem. Phys. Lett.* **1995**, *245*, 448.
(131) Bonacic-Koutecky, V.; Bruckmann, P.; Hiberty, P.; Koutecky, J.; Leforestier, C.; Salem, L. *Angew. Chem., Int. Ed. Engl.* **1975**, *14*, 575.
(132) Salem, L. *Science* **1976**, *191*, 822.
(133) Brooks, B. R.; Schaefer, H. F. III. *J. Am. Chem. Soc.* **1979**, *101*, 307.
(134) Buenker, R. J.; Bonacic-Koutecky, V.; Pogliani, L. *J. Chem. Phys.* **1980**, *73*, 1836.
(135) Sension, R. J.; Hudson, B. S. *J. Chem. Phys.* **1989**, *90*, 1377.
(136) Pullen, S. H.; Anderson, N. A.; Walker, L. A.; Sension, R. J. *J. Chem. Phys.* **1997**, *107*, 4985.
(137) Lochbrunner, S.; Fuss, W.; Schmid, W. E.; Kompa, K.-L. *J. Phys. Chem.* **1999**, *102*, 9334.
(138) Farmanara, P.; Stert, V.; Radloff, W. *Chem. Phys. Lett.* **1998**, *288*, 518.
(139) Woodward, R. B.; Hoffmann, R. *Angew. Chem., Int. Ed. Eng.* **1969**, *8*, 781.
(140) Goddard, W. A., III. *J. Am. Chem. Soc.* **1970**, *92*, 7520.
(141) Goddard, W. A., III. *J. Am. Chem. Soc.* **1972**, *94*, 793.
(142) Zimmerman, H. E. *Acc. Chem. Res.* **1971**, *4*, 272.
(143) Houk, K. N.; Gonzalez, J.; Li, Y. *Acc. Chem. Res.* **1995**, *28*, 81.
(144) Bernardi, F.; Bottoni, A.; Olivucci, M.; Venturini, A.; Robb, M. A. *J. Chem. Soc., Faraday Trans.* **1994**, *90*, 1617.
(145) Wiest, O.; Montiel, D. C.; Houk, K. N. *J. Phys. Chem.* **1997**, *101*, 8378.
(146) Leigh, W. J. *Can. J. Chem.* **1993**, *71*, 147.
(147) Lawless, M. K.; Wickham, S. D.; Mathies, R. A. *J. Am. Chem. Soc.* **1994**, *116*, 1593.
(148) Lawless, M. K.; Wickham, S. D.; Mathies, R. A. *Acc. Chem. Res.* **1995**, *28*, 493.
(149) Saltiel, J.; Lim, L.-S. *J. Am. Chem. Soc.* **1969**, *91*, 5404.
(150) Lord, R. C.; Rea, D. G. *J. Am. Chem. Soc.* **1957**, *79*, 2401.

(151) Craig, N. C.; Borick, S. S.; Tucker, T.; Xia, Y.-Z. *J. Phys. Chem.* **1991**, *95*, 3549.
(152) Negri, F.; Orlandi, G.; Zerbetto, F.; Zgierski, M. Z. *J. Chem. Phys.* **1995**, *103*, 5911.
(153) Wiberg, K. B.; Rosenberg, R. E. *J. Phys. Chem.* **1992**, *96*, 8282.
(154) Gross, E. K. U.; Kohn, W. *Adv. Quantum Chem.* **1990**, *21*, 255.
(155) Lam, B.; Schmidt, M. W.; Ruedenberg, K. *J. Phys. Chem.* **1985**, *89*, 2221.
(156) Thompson, K.; Martínez, T. J. *J. Chem. Phys.* **1998**, *110*, 1376.
(157) Eckert, F.; Werner, H.-J. *Chem. Phys. Lett.* **1999**, *302*, 208.
(158) Warshel, A.; Levitt, M. *J. Mol. Biol.* **1976**, *103*, 227.
(159) Thompson, M.; Schenter, G. K. *J. Phys. Chem.* **1995**, *99*, 6374.
(160) Ben-Nun, M.; Martínez, T. J. *Chem. Phys. Lett.* **1998**, *290*, 289.
(161) Dunning, T. H. J. *J. Chem. Phys.* **1989**, *90*, 1007.
(162) Woon, D. E.; Dunning, T. H. *J. Chem. Phys.* **1993**, *98*, 1358.
(163) Szabo, A.; Ostlund, N. S. *Modern Quantum Chemistry*; McGraw-Hill: New York, 1989.